Available online at www.CivileJournal.org

Civil Engineering Journal

Vol. 6, No. 12, December, 2020

Prediction of Ground Settlement Induced by Slurry Shield Tunnelling in Granular Soils

Mo'men Ayasrah [a*], Hongsheng Qiu [b], Xiedong Zhang [b], Mohammad Daddow [b]

[a] *Communication and Transportation Engineering, School of Transportation, Wuhan University of Technology, 430063 Wuhan, China.*

[b] *Road and Railway Engineering, School of Transportation, Wuhan University of Technology, 430063 Wuhan, China.*

Received 10 September 2020; Accepted 20 November 2020

Abstract

Underground structures play an important role in achieving the requirements of rapid urban development such as tunnels, parking garages, facilities, etc. To achieve what is needed, new transportation methods have been proposed to solve traffic congestion problems by using of high-speed railway and subway tunnels. One of the issues in urban spaces due to tunnel excavation is considerable surface settlements that also induce problems for surface structures. There are a variety of published relationships concerned with field measurements and theoretical approaches to evaluating the amount of the maximum surface settlement value due to tunneling. This paper studies the ground surface settlement caused by the Greater Cairo Metro – Line 3 - Phase-1. This project was constructed by a slurry shield Tunnel Boring Machine (TBM). Therefore, this work consists of two parts. The first part presents the details of the project and monitoring results field and laboratory geotechnical investigations in order to determine the soil properties. The second part is to the comparison between the field measurements and theoretical approaches for surface settlement due to tunneling construction. At the end of the works, the results show that the more convenient methods which approach the field measurements, and the major transverse settlement occurs within the area about 2.6 times the diameter of the tunnel excavation.

Keywords: Tunnel Excavation; Surface Settlement; Field Measurements; Theoretical Approaches; Tunnel Boring Machine.

1. Introduction

Underground structures play an important role in achieving the requirements of rapid urban development such as tunnels, parking garages, facilities, etc. To achieve what is needed, new transportation methods have been proposed to solve traffic congestion problems by using of high-speed railway and subway tunnels [1]. For instance, Line 3 of Cairo metro meets huge transportation demands along the route, and reduces the traffic density at the other means of transportation with a rate equivalent to 2 million trips/daily. However, the construction of tunnel induces ground movements, both vertical and lateral, causing surface subsidence, curvature change, inclination, and discontinuous deformation, which in turn affect the safety and stability of adjacent existing buildings within the settlement range of strata, thus bringing potential safety obstacles to the building structures [2-9].

It is well-acknowledged that the soil movement occurring during deep excavation process plays a significant role in this regard. Excessive soil movement causes excessive settlements of nearby buildings and may cause different damages [10]. However, in reality, ground movements depend on a number of factors such as: behavior of the soil around tunnel,

* Corresponding author: momen_992@yahoo.com

http://dx.doi.org/10.28991/cej-2020-03091617

geometry of tunnel and depth, tunnel construction method, the quality of the workmanship and management [11, 12]. This emphasize that the ground movements and the depth of tunnel is neither simple nor nonlinear relationship [13].

Several approaches, such as the empirical method, centrifugal method, numerical simulation method, and field monitoring, have been used to predict the surface settlement during the shield tunneling. Peck (1969) [14] used the results of monitoring program to predict the deformations and stresses related with construction of tunnel and deep excavation. Since then, ground movements have been determined by investigations of many empirical and semi-empirical methods. These methods do not take into account the building effects and therefore they measure only the greenfield deformations. However, the empirical and semi-empirical methods considered the initial important phase in predicting the excavations effect on close buildings.

The increase of the surface settlement may cause more buildings to be damaged or influence the serviceability of the buildings [15-17]. Therefore, to control tunneling induced deformation on the buildings in the nearby area within the allowable limit is an important task for engineers involved in a tunneling project. The damage to an existing building can be caused by excessive settlement [16]. To date, in spite of the recent advances made in assessing the stability and effects of excavations on nearby properties, structures failures or adjacent roadway, the serviceability problems such as cracking of structural or architectural elements, uneven flooring, or inoperable windows and doors due to the vertical settlement and lateral deformations caused by deep excavations are much more common than failures [18]. Recently on July 2020, one of the most examples of such damage to corners of building number 17 on Brazil Street in Zamalek as well as at the front yard and fence of the adjacent Bahraini embassy caused by the slight ground subsidence that occurred. The subsidence was due to the result of ongoing excavation works in the line 3 - phase 3 of the metro undergoing in Zamalek district.

The Greater Cairo Metro, Line 3, Phase-1 starts from El-Attaba Station to El-Abbasia Station and crosses very close to a multi-story carparking building founded on piles namely, El-Attaba Garage. Considering that the underground construction might cause damages to the building, the survey before the construction and prevention and monitoring measures during and after the construction were carried out. This work consists of two parts. The first part presents the details of the project and monitoring results field and laboratory geotechnical investigations in order to determine the physical soil properties of the site which helps in predicting the behavior of the soil and the settlement that occurring on adjacent El-Attaba Garage building due to construction of tunneling. The second part is to comparison between the field measurements and theoretical approaches for surface settlement.

The remainder of this paper is organized as follows. Section 2 presents the details of the case study. In Section 3, the site investigations are explained. The stages of construction are demonstrated in Section 4. Section 5 presents the theoretical methods of ground surface settlement. The computational results are presented and analyzed in Section 6. Finally, Section 7 presents conclusions and suggestions for future research. The research flowchart is shown in Figure 1.

2. Case Study

One of the Egyptian mega projects established to solve many traffic problems that have been recently raised is the Greater Cairo Underground Metro project. The Greater Cairo Metro-Line 3 was constructed by a slurry shield Tunnel Boring Machine (TBM), with 9.55 m a diameter. The tunnel has an external and internal diameter with 9.15 m and 8.35 m respectively. The precast segmental lining thickness of 0.4 m. This line is 47.87 km length starts from Imbaba to Cairo airport; also, as planned, it is going to be constructed in four phases. In this study, The Greater Cairo Metro – Line 3 - Phase-1 moves underground from El-Attaba to El-Abbasia stations was considered to understand performance of tunnel system and the expected ground movement during tunneling construction that passes through soil layers. This Phase is 4.3 km length and consists of 5 underground stations and 4 annexed structures, as shown in Figure 2.

El-Attaba Garage building is 77.04 m-length and 45.55 m-width. It is founded near the greater Cairo metro-line 3-phase-1, constructed with 8 stories as shown in Figure 3. This building is 6.45 meters from the center of the tunnel and making an angle of about 42° from the tunnel as shown in Figure 4. The building was supported by 245 non-displacement concrete piles arranged in pile caps group. The pile dimensions are 0.6m in diameter and 20m length and passes through layered soil.

As reported in National Authority for Tunneling (NAT), several instrumentations were used to monitor the predicted ground movements of the soil during tunnel progress. The five measured vertical Surface Settlement Points (SSP.b, SSP.c, SSP.d, SSP.e and SSP.f) were installed around the Garage El-Attaba building as shown in Figure 3. Through the tunnel advancement from July 2010 to August 2010, the building was monitored at the location of surface settlement points and an Elevation Reference Point (ERP.a).

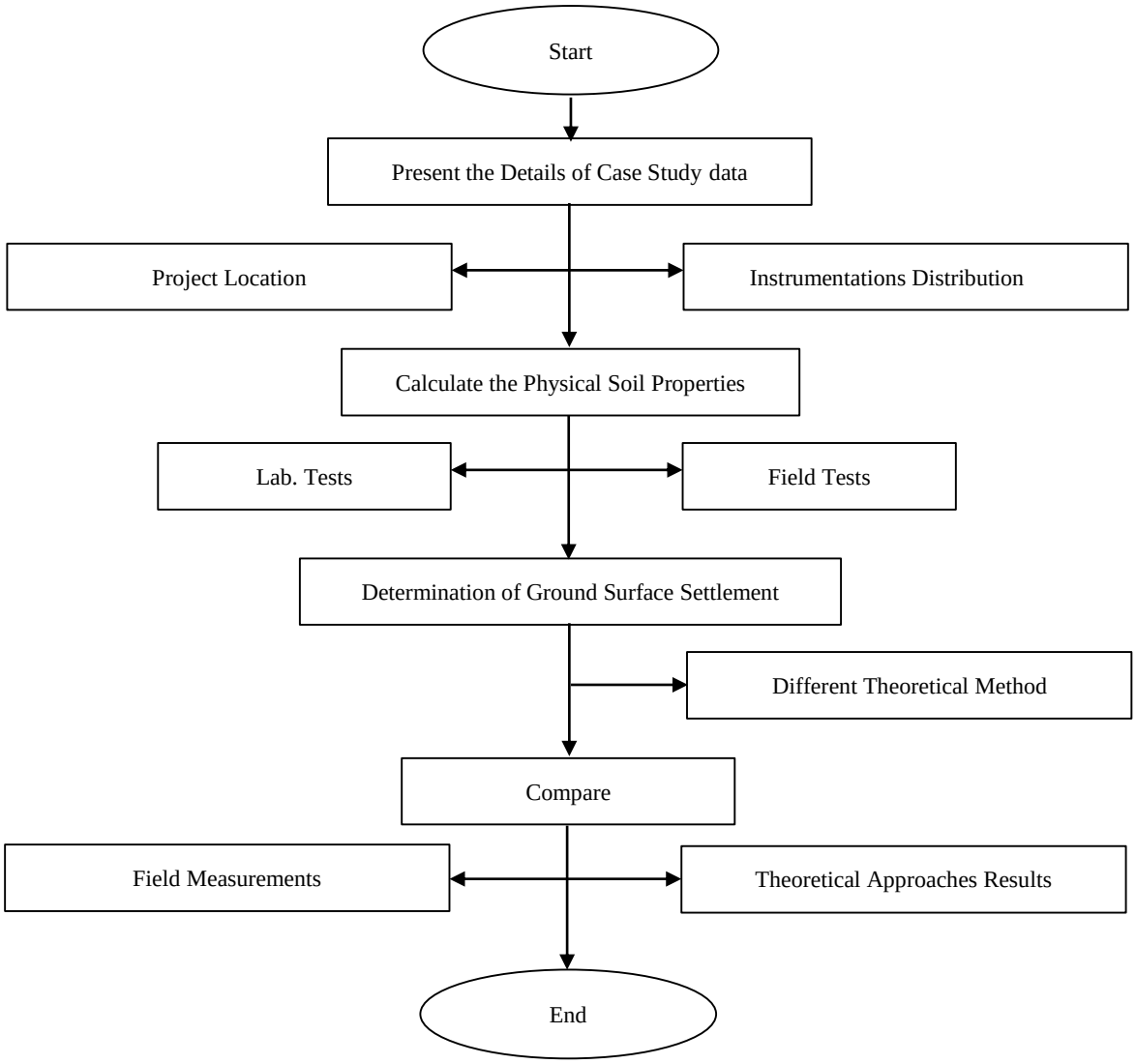

Figure 1. Flowchart of the present study

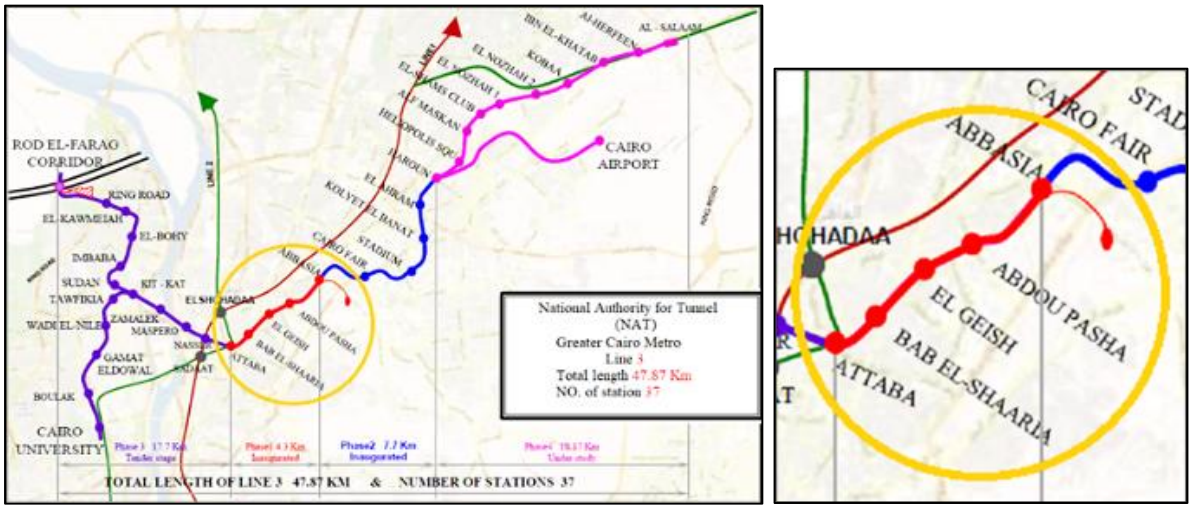

Figure 2. (a) The Greater Cairo Metro -Line 3, after National Authority for Tunnelling; (b) Zone of the study [19]

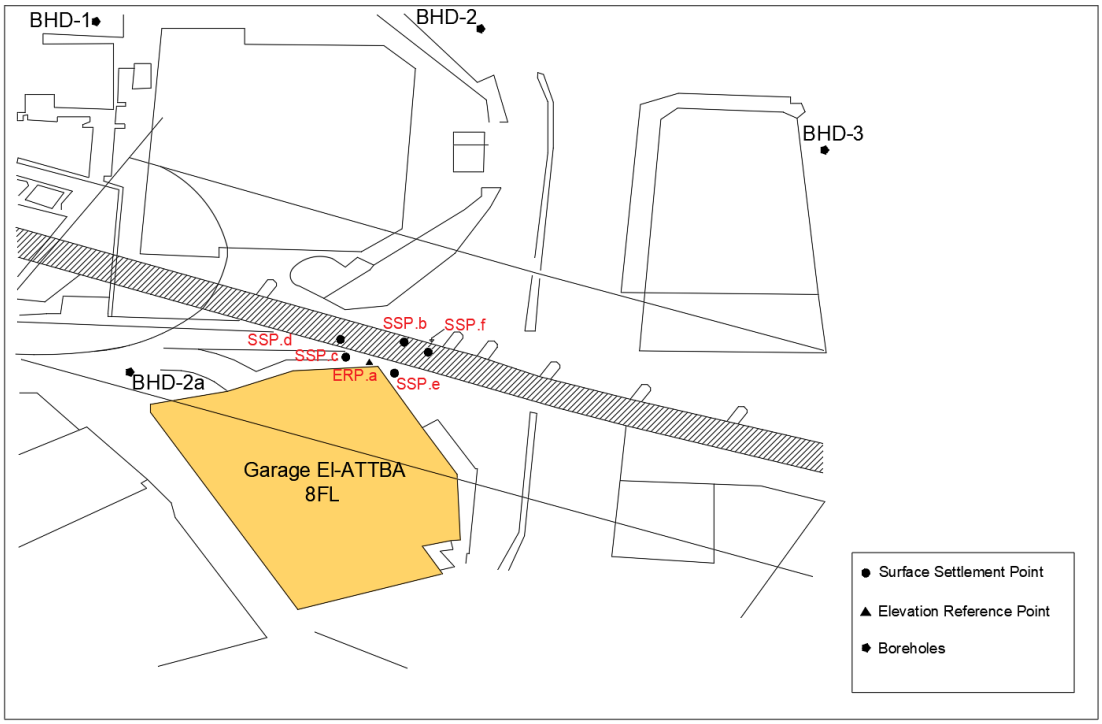

Figure 3. Garage El-Attaba location according to Greater Cairo Metro and instruments system layout [19, 20]

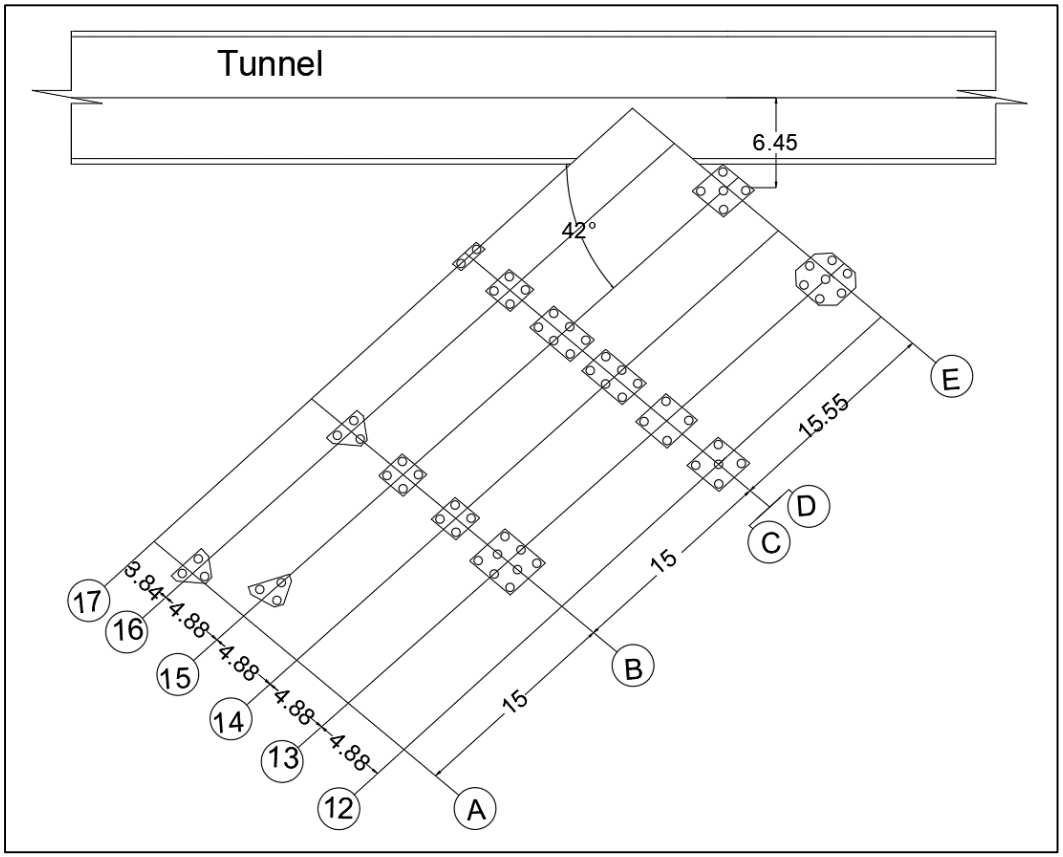

Figure 4. The pile caps location to the tunnel route. Units in (m)

3. Site Investigations

Referring to geotechnical investigation of the Greater Cairo Metro – Line 3- Phase-1, thirteen boreholes and standard penetration tests [20], were carried out with a vary depths from (24 to 70) m and different locations along the phase-1 as indicated in Figure 5.

Figure 5. The boreholes locations along phase-1 and near Garage El-Attaba building

The thirteen boreholes were performed using mechanical rotary drilling fluid (using bentonite) techniques. This research focused on the boreholes that located at the first station (from El-Attaba to Bab- El-Shaaria) near the El-Attaba Garage building. After review these boreholes, it's found there is consistent with soil description but difference with the level of depth. As shown in Figure 3. borehole No. 2A is nearest to Garage El-Attaba building, thus the soil cross section at this borehole was taken as representative to soil profile in this study:

3.1. Soil Profile at Borehole No. 2A

Figure 6 shows the soil profile section at borehole No. 2A with a depth of 70 m. The groundwater existed at an average depth of 1.65 m below the ground surface. The soil properties, thickness, and others parameters are descripted in the following sections.

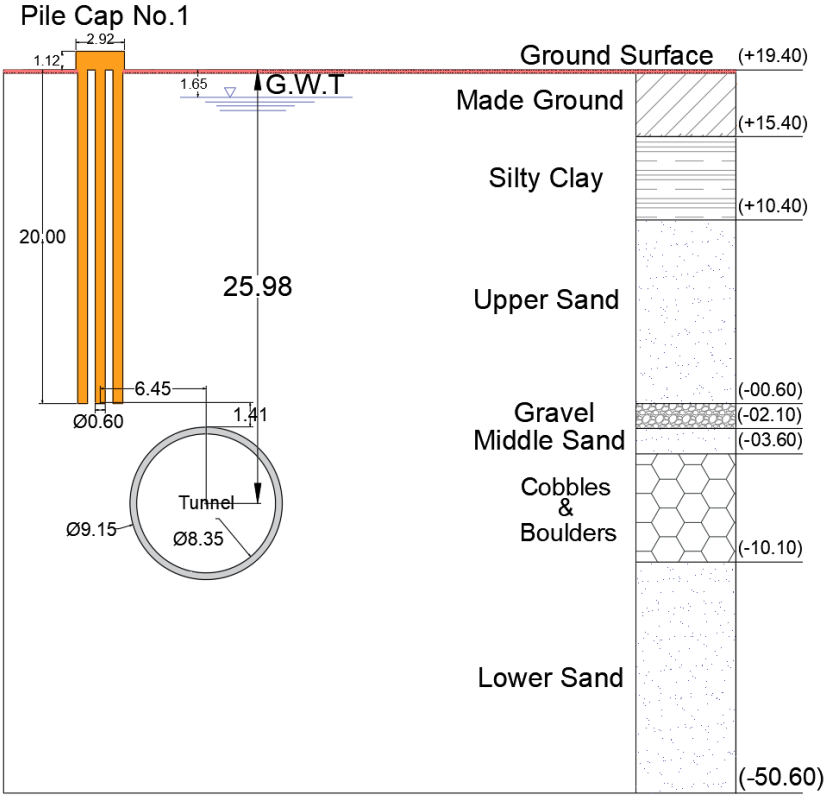

Figure 6. Soil profile at the location of BHD. 2A. Units in (m) [20]

3.2. Soil Layers Properties

3.2.1. In-Situ Field Test and Soil Properties

3.2.1.1. Standard Penetration Test (SPT)

In this study and according to the Egyptian code of practice [21], there are many required corrections such as: (overburden effect, underground water table and the borehole diameter effect) were taken into account to measure the N-corrected value in order to classify the soil and determine the friction angle as listed in Table 1. In the same line, the friction angle, ø are estimated by Peck et al. (1953), Guiliani and Nicoll (1982) and Wolff (1989) [22-24] for cohesionless soil layers as shown in Figure 9.

Table 1. Obtained soil parameters using SPT corrected values

Layer	N_{30}	$N_{correct}$	Friction Angle
Made Ground	-	-	-
Silty Clay	-	-	-
Medium to Dense sand	45	39	36-40
Gravel	>50	74	>40
Silty Sand	42	31	36-40
Cobbles & Boulders	>50	74	>40
Dense Sand	>50	49.3	>40

As shown in the summary at the end of this section, and based on SPT-N value, the Young's modulus, E for sandy soil layers are estimated using theoretical equations by Webb (1969); Bowles (1982) and Denver (1982) [25-27]. In addition, The Young's modulus for coarse soil layers, are obtained using the SPT original N-values according to the following recommended correlations by ECP 202/3 (2005) [28];

For silty sand soil,

$$E_s = 4N \ \left(\frac{Kg}{cm^2}\right) \quad (1)$$

For medium to fine sand soil,

$$E_s = 7N \ \left(\frac{Kg}{cm^2}\right) \quad (2)$$

For dense sand soil,

$$E_s = 10N \ \left(\frac{Kg}{cm^2}\right) \quad (3)$$

For gravelly sand and gravel soil,

$$E_s = 12N \ \left(\frac{Kg}{cm^2}\right) \quad (4)$$

3.2.2. Laboratory Test

3.2.2.1. Grain-Size Distribution

To classify the soil properly, the grain-size distribution of coarse-grained soil is generally determined by means of sieve analysis. Table 2 shows the sieve analysis test results. The soil stratification at location of BHD. 2A can be summarized as follows: Layer (1) starts at level (+19.40) and extends to level (+15.40), and it is a made ground layer consisting of 30% stone pieces and red bricks, and 70% clay. Layer (2) begins from level (+15.40) to level (+10.40), and it consists of firm to stiff brown micaceous clay. Layer (3) is a thick segment of silty poorly graded sand that starts from level (+10.40) to level (-00.60) with a thickness of 11.0 m. Layer (4) starts from level (-00.60) to level (-2.10), and it consists of yallowish brown slightly sand poorly graded gravel. Layer (5) starts from level (-2.10) to level (-3.60), and it consists of dense yallowish brown micaceous slightly gravelly silty poorly graded sand with little calcareous materials. Layer (6) starts from level (-3.60) to level (-10.10), and it contains of hard formation consist of cobbles and boulders. The last layer is very dense yallowish brown calcareous slightly silty poorly graded sand extended to the end of boring. The permeability coefficient of sand soil layers was estimated from sieve analysis test results using (Equation 4) [29]:

$$K_{per} = C \times D_{10}^2 \quad (5)$$

Where,

K_{per} = Coefficient of permeability (cm/sec)

C = Constant, typically assumed to be 100.
D_{10} = Grain size corresponding to 10% by weight passing, also referred to as the effective size (mm).

Table 2. Sieve analysis test results

Layer	Depth	Sample	D_{60}	D_{30}	D_{10}	C_u	C_c	K_{per}
Medium to Dense sand	9.00-10.00	Ds-9	0.2	0.08	0	-	-	0
	13.00-13.45	Ds-14	0.5	0.35	0.235	2.13	1.04	5.53
	17.50-17.95	Ds-20	0.45	0.28	0.17	2.65	1.02	2.89
Silty Sand	21.50-21.95	Ds-24	0.4	0.2	0	-	-	0
Dense Sand	30.00-30.27	Ds-27	0.6	0.38	0.19	3.16	1.27	3.61
	33.50-33.76	Ds-29	0.6	0.39	0.17	3.53	1.49	2.89
	37.00-37.28	Ds-31	0.45	0.32	0.16	2.81	1.42	2.56
	40.50-40.77	Ds-33	0.49	0.34	0.194	2.53	1.22	3.76
	44.00-44.09	Ds-35	0.53	0.3	0.16	3.31	1.06	2.56
	47.50-47.66	Ds-37	0.57	0.39	0.265	2.15	1.01	7.02
	51.00-51.14	Ds-39	0.43	0.3	0.172	2.5	1.22	2.96
	54.50-54.95	Ds-41	0.4	0.24	0.145	2.76	0.99	2.10
	58.00-58.09	Ds-43	0.9	0.62	0.322	2.80	1.33	10.37
	61.50-61.53	Ds-45	0.5	0.32	0.19	2.63	1.08	3.61
	65.00-65.13	Ds-47	0.41	0.3	0.166	2.47	1.32	2.76
	69.00-69.13	Ds-49	0.41	0.28	0.156	2.63	1.23	2.43

D_{60} = Diameter corresponding to 60% by weight passing, indicated by the gradation curve at the 60% passing level (mm),
D_{30} = Grain size, indicated by the gradation curve at the 30% passing level (mm),
C_U = Uniformity coefficient (D_{60}/D_{10}), and
Cc = Curvature coefficient of the gradation curve ($D_{30}^2/D_{60} * D_{10}$).

3.2.2.2. Water Content and Atterberg Limits

There are three clay samples were taken from BHD. 2A at vary depths of 4.0, 5.0 and 7.50 m underground surface to estimate the Atterberg limits and water content that is necessary to classify the cohesive soil. Also, the relative consistency (I_c) was estimated by using the following equation (Equation 6) [30], and based on the relative consistency values, the soil classified and the undrained cohesion for each clay sample were determined and given in Table 3.

$$I_c = \frac{L.L - W.c}{I_p} \quad (6)$$

Where,

$L.L$ = soil liquid limit (%),
$w.c$ = soil water content (%), and
I_p = plasticity index.

Table 3. Water content and Atterberg limits test

Sample level (m)	W.C %	L.L %	P.L %	I_c	Clay Classification	C_u (kN\m^2)
4.00-5.00	32	51	27	0.79	Stiff Clay	50-100
5.00-6.50	41	81	34	0.85	Stiff Clay	50-100
7.30-9.00	34	48	27	0.67	Medium Stiff	25-50

3.2.2.3. Consolidation Test

Consolidation test was conducted on clay soil samples taken from site at depth of (8.00-8.30) m underground surface. Figure 7 shows the e-Log P curve for consolidation test. Three pressure increments (56.81-111.80, 111.80-166.78, and 166.78-221.77) kN/m^2 were applied on this sample. Based on test results, the average soil volume compressibility

coefficient, mv was determined with value of (9.29E-05) m^2/kN. Then, clay soil constrained modulus, E_s was estimated to be 1.10E+04 kN\m^2 using (Equation 7):

$$E_s = \frac{1}{m_v}\left(\frac{Kg}{cm^2}\right) \quad (7)$$

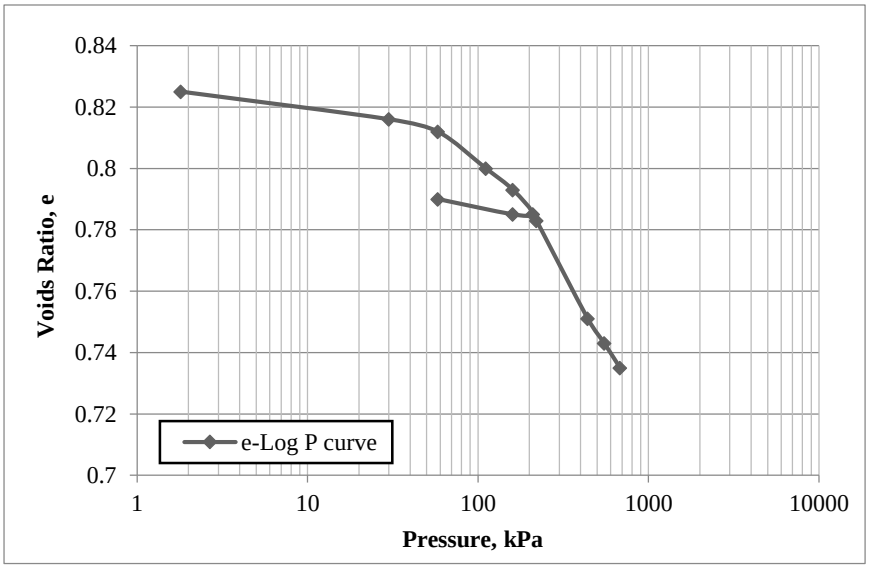

Figure 7. The relationship between the pressure and voids ratio in consolidation test (e-Log P curve)

3.2.2.4. Unconfined Compression Test

The unconfined compression test is a special type of unconsolidated undrained triaxial test, UUT. The soil undrained shear strength, q_u was estimated. Also, the undrained shear strength (C_u or S) and the undrained Young's modulus (E_u) of the cohesive soil layer are calculated using (Equations 8 and 9), respectively. Table 4, display measured values of (q_u) for clay samples at variable depths using the unconfined compression test.

$$S = C_u = \frac{q_u}{2}\left(\frac{Kg}{cm^2}\right) \quad (8)$$

$$E_u = k\, C_u \quad (9)$$

Where; k is estimated using Duncan chart [31].

Table 4. Unconfined compression test results

Depth (m)	Undrained Shear Strength (q_u) kN/m^2	Undrained Cohesion (C_u) kN/m^2	Undrained Young's Modulus (E_u) kN/m^2	Clay Classification
5.00-6.50	220	111	27750	Very Stiff Clay
6.50-7.50	140	70	17500	Stiff Clay
7.50-9.00	100	50	12500	Stiff Clay

3.2.2.5. Direct Shear Test

A direct shear device is used to determine the shear strength indicated by Cohesion (C) and Angle of Internal Friction (ø) of any soils. Many calculations depend on these two parameters such as; bearing capacity measurements at any depths, slopes design, and to calculate the consolidation parameters and in many other analyses. Figure 8 shows the shear stress and shear displacement for 12 m and 35 m depth, respectively.

The Figures 9 to 11 show the summery of values of the soil's physical properties such as friction angle, young's modulus, and cohesion at different depth of BHD.2A, which were calculated in this study from laboratory, field tests and theoretical equations of previous studies as mentioned above. Also, it must be mentioned that, in this case study, the Young's modulus and the friction angle for (sand, gravel, and boulders) layers are taken based on ECP code measurements. On the other hand, the clay soil properties (un-drained shear strength, C_u and undrained young's modulus, E_u are taken from unconfined compression test. Table 5 shows the soil parameters that are used in this study to measure the ground surface settlement.

Table 5. Soil layers properties

Layers	Made ground	Silty Clay	Medium to Dense sand	Gravel	Silty Sand	Cobbles & Boulders	Dense Sand
Thickness, (m)	4	5	11	1.5	1.5	6.5	extended
Young Modulus, E, (kN/m^2)	40000	27750	31185	121210	16475	121210	70706
Unit Weight γ, (kN/m^3)	17	18.25	17.70	20	19.23	21	18.34
Friction angle, ϕ^o	27	0	36	41	36	41	40
Cohesion, C (kN/m^2)	-	C_u=111	-	-	-	-	-
Poisson's Ratio, ν	0.3	0.3	0.3	0.3	0.3	0.3	0.3
Lateral earth pressure, K	0.546	1	0.384	0.343	0.370	0.343	0.357

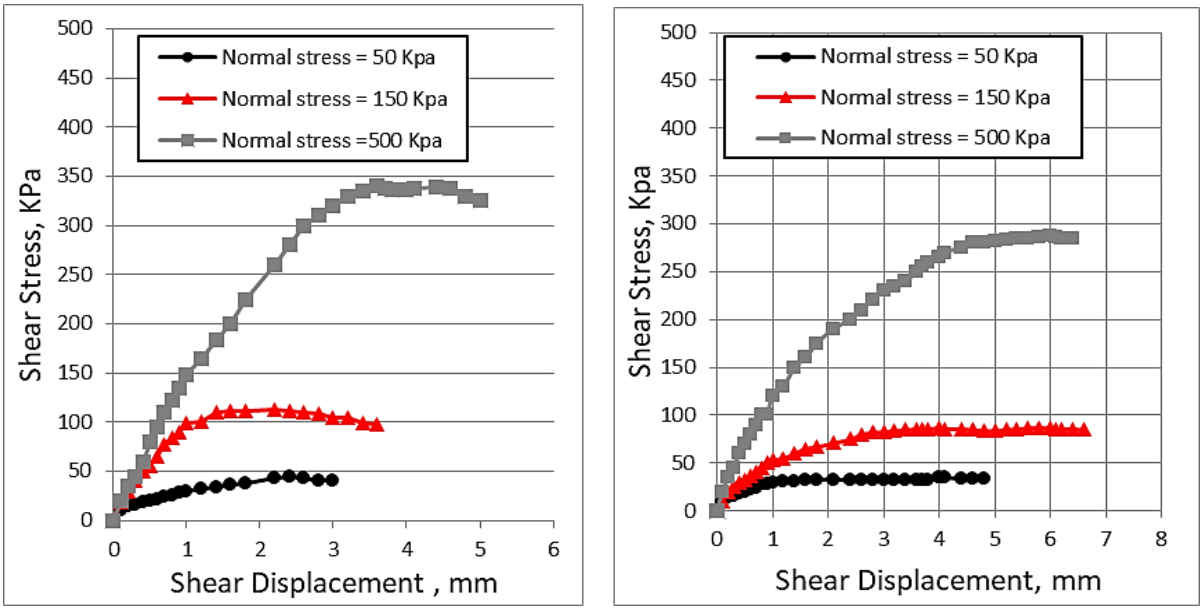

Figure 8. The relationship between the shear displacement and shear stress for uncompressing test at a) 12m and b) 35m depths

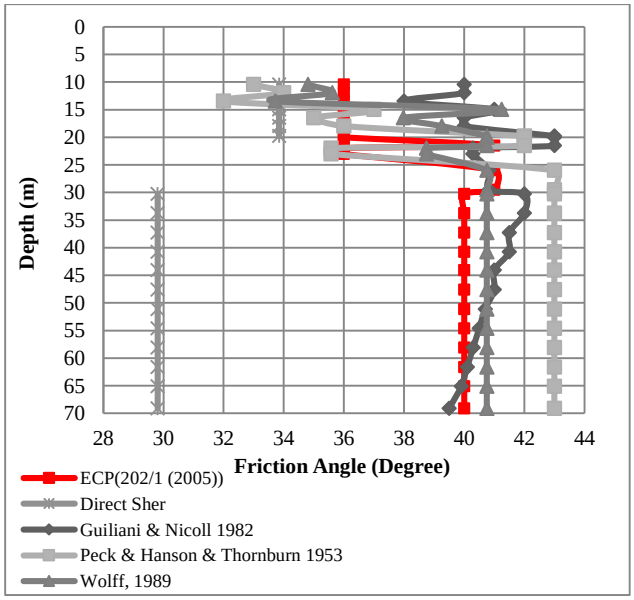

Figure 9. The relation between friction angles and different depths for BHD.2A

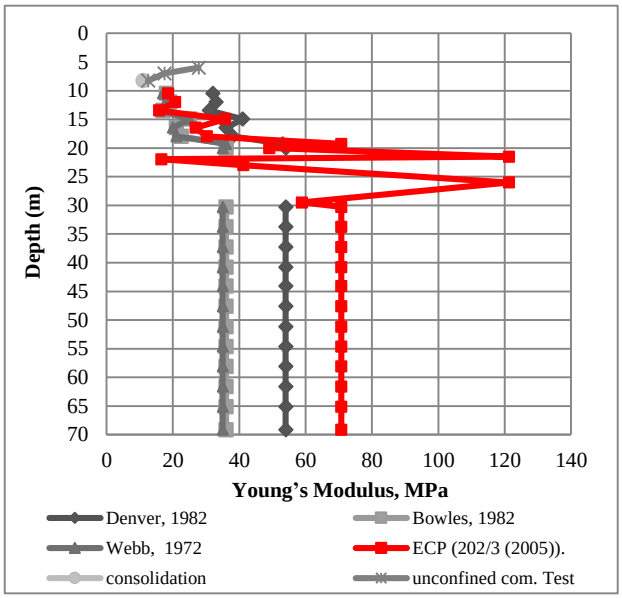

Figure 10. The relation between young's modulus and different depths for BHD.2A

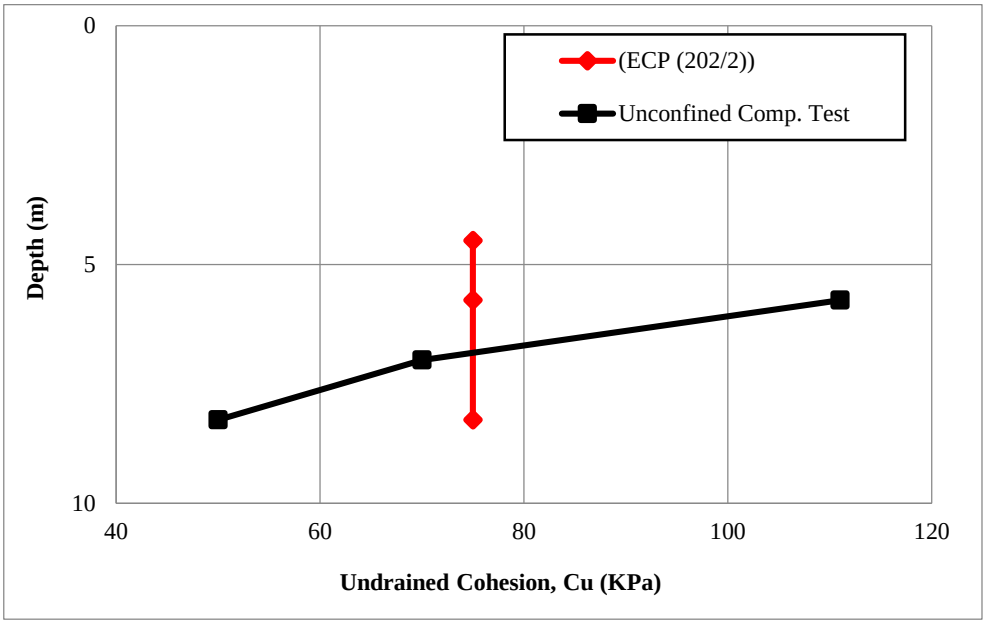

Figure 11. The relation between the undrained shear strength and different depths for clay layer at BHD.2A

4. Stages of Construction

In the construction of the Greater Cairo Metro, line-3, slurry shield was used to execute utilizing of 9.55 m external diameter. The length of TBM is 9 m with a tail piece thickness 5 cm. According to NAT., the rate of TBM advance is ranging from (6 to 13) m/day. Figure 12 describes the sequence followed in the construction of the tunnel. Six stages of construction were adopted as follows: The objective function of the model is given as follows:

a) 1st Stage: Starts with boring a vertical pit.

b) 2nd Stage: A cylindrical excavator called a "tunnelling shield" is brought in through the vertical pit and assembled.

c) 3rd Stage: The machine starts excavation toward the adjacent vertical pit. The tunnelling shield presses and rotates its cutting wheel at the front against soil to excavate.

d) 4th Stage: The machine excavates and moves forward as hydraulic jacks at the back stabilized it. Once a certain distance is excavated the machine folds the jacks in and install a ring-shaped concrete wall called a segment.

e) 5th Stage: The grouting is acted on the perimeter of the segments toward the soil.

f) 6th Stage: The machine builds the tunnel by repeating the process of precasting the segment extending the jacks, then folding the jacks in and precasting the segment. When the machine reaches the next vertical pit, it is removed to complete the underground tunnel.

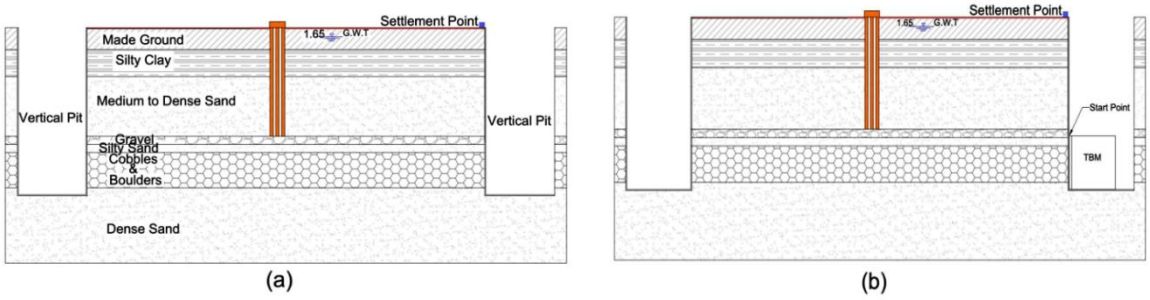

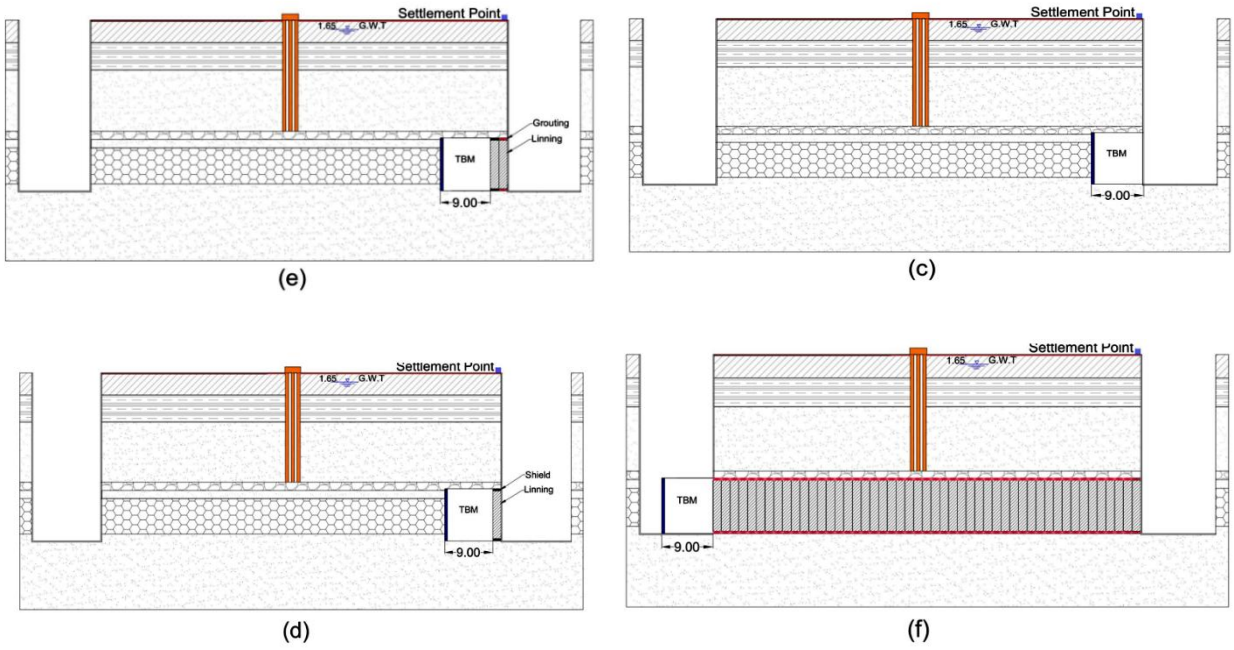

Figure 12. Stages construction of tunnel case study; (a) Stage 1: Starts with boring a vertical pit, (b) Stage 2: Assemble the TBM at the vertical pit, (c) Stage 3: The machine starts excavation toward the adjacent vertical pit, (d) Stage 4: The machine excavates and moves forward and constructed the segment, (e) Stage 5: The grouting is acted on the perimeter of the segments toward the soil, and (f) Stage 6: Repeating the process of precasting the segment up to the TBM arrives in the next vertical pit to be dismantled for transportation.

5. Theoretical Calculation of Surface Settlement

The ground movements estimation is the first step to proceed a reliable risk-assessment of the potency effects on buildings and underground structure, which is necessary for the tunneling design of in urban regions. There are many research examples clarifying the characteristics of ground movement when a tunnel is excavated. The maximum settlement amount (S_{max}) and the position of the inflection point (i) are indicated by a normal distribution curve (Gaussian distribution curve) on the form of subsidence on the cross-section of the tunnel, as shown in Figure 13.

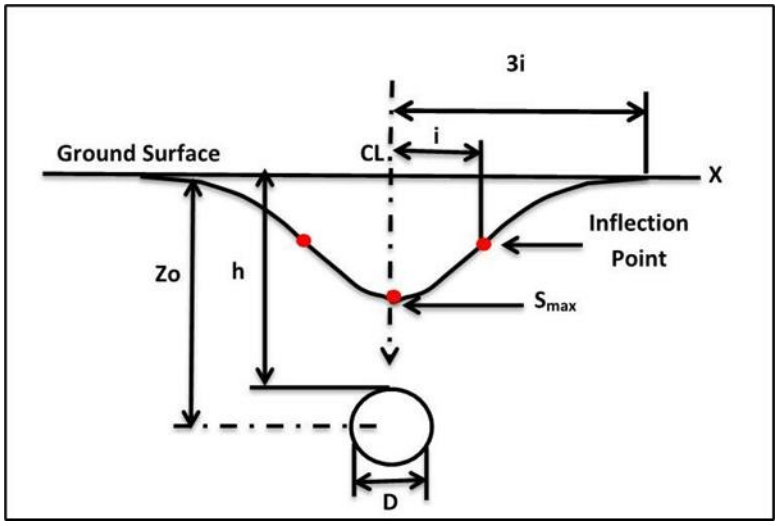

Figure 13. Definition of settlement profile of Gaussian form, after Peck 1969 [13]

For the case of a single tunnel, the development of the surface settlement trough is estimated by various methods as follows:

1. Peck (1969) [14], summarized a large number of measured data to describe the surface settlement caused by construction of a shield tunneling and expressed that surface settlement approximate normal distribution and proposed the Peck formula as follows:

$$S_{(x)} = S_{max} * exp\left(-\frac{x^2}{2i^2}\right) \quad (10)$$

Where

$S_{(x)}$ = the surface settlement,
x = the horizontal distance from tunnel centreline,
S_{max} = the maximum settlement on the tunnel centreline, and
i = the inflection point position.

Settlement due to tunnelling is usually realize by a dimensionless parameter that is called Ground Loss or Volume Loss. Volume loss is defined as the proportion of excavation area volume to initial volume of the tunnel per unit length of excavation [32], modified the Gaussian distribution based on many in-situ measurements and centrifuge test. By integrating Peck's Gaussian relationship, the volume of settlement trough, V_s can be estimated.

$$V_s = \int_{-\infty}^{+\infty} S_v dx = \sqrt{2\pi} i_x S_{max} \quad (11)$$

Mair et al. (1982) [32], suggested the following equation to measure the maximum surface settlement:

$$S_{max} = \frac{V_s}{\sqrt{2\pi} i} = 1.252 \frac{V_L R^2}{i} \quad (12)$$

Where;

V_s $= \pi R^2 V_L$
R = the radius of tunnel

This formula is needed to determine two parameters for the prediction of settlement: the volume loss (V_L) and the inflection point position (i). The volume loss (V_L) depends on tunneling techniques and the soil behaviors, and it is almost obtained through measurements or local experiences and it ranges between (0.5-1%) for shield tunnel boring machine. The technical data of the employed TBM recommended the total volume loss as 0.5%. The inflection point position (i) determines the influence domain of settlement and plays a main role in the settlement amount when the volume loss is constant, the value of the inflection point position (i) is related to the nature soil formation, the tunnel depth, and the tunnel radius.

O'Reilly and New (1982) [33] were presented more generalized empirical equations of the profile settlement depends on the Peck's research. They developed the general trough width equation for all soil types for multi-layered strata (N layers) as the following equation:

$$i_n = K_1 Z_1 + K_2 Z_2 + K_3 Z_3 + \cdots + K_n Z_n \quad (13)$$

Where; i is the width of the settlement trough; K is a parameter depending only on the nature of soil. Field data during tunnelling collected all over the world indicate that K varies between 0.4 and 0.6 for stiff clays, between 0.6 and 0.75 for soft clays, and between 0.2 and 0.45 for sands and gravels, Mair and Taylor 1997 [34], regardless the size and method of the tunnel.

2. The Oteo Method

This semi-empirical method is based on Oteo's works over the last 30 years Oteo and Moya (1979) [35] and Sagaseta et al. (1980) [36], which allows estimating the settlement along the perpendicular to the axis of the tunnel. In general, this method is a modification of the Peck method, in which more parameters of the tunnel and the mass containing it are used:

$$S_{max} = \Psi \times \frac{\gamma D^2}{E} \times (0.85 - \mu) \quad (14)$$

Where,

μ = Poisson's ratio,
γ = The total unit weight of the soil,
D = The tunnel diameter,
Ψ = An empirical parameter to be obtained from monitoring data analysis and equal to 0.4~0.5, and
E = The tensile modulus of elasticity.

3. Limaniv's Method

Limaniv (1957) [37] has presented the theoretical methods proceed from the assumption of elastic behavior of the soil surrounding the tunnel to calculate the surface settlement resulting from the construction of tunnels or mine excavations. The Limaniv's relationship for computing the maximum settlement is as follows:

$$S_{max} = (1 - v^2)\frac{P}{E}\left[\frac{4r_o^2 h_0}{h_0^2 - r_0^2}\right] \quad (15)$$

Where;

v = Poisson's ratio,

E = Young's modulus,

r_0 = Tunnel radius,

h_0 = Tunnel depth, and

P = Radial load that can be expressed as;

$$P = \sigma_z \frac{1 + K_r}{2} \quad (16)$$

Where,

σ_z = The vertical stress in tunnel centreline and

K_r = Lateral earth pressure.

4. The Sagaseta Method

The equation of the maximum surface settlement is calculated based on the analytical solution given by Sagaseta 1987 [38] and later modified by Sagaseta 1988 [39] and Uriel and Sagaseta 1989 [40], and expressed as:

$$S_{max} = \frac{V_s\, H}{\pi\,(x^2 + H^2)} \quad (17)$$

Where,

H = Tunnel axis depth,

x = Distance to the centre line, and

V_s = Volume of settlement trough.

5. The Ecrelebi Method

Ecrelebi (2005) [41], presented the following relationship for estimating the maximum surface settlement over the tunnel axis:

$$S_{max} = 0.785 \times \gamma \times h_0 \times \frac{4 \times R^2}{i \times E} \quad (18)$$

Where,

h_0 = Tunnel axis depth

R = Tunnel radius

γ = Unit weight (ton/m^3), and

E = Elasticity modulus (ton/m^2), which is the weighted average for layers in this study.

6. Results and Discussion

In this section, the ground surface settlement due to tunneling was calculated with the theoretical methods and compared with field data measurements. Figure 14 shows the transverse settlement trough of the ground surface. The results indicate that the settlement obtained by Oeto and Mair methods and the monitoring results match well with the Gauss distribution. From the Oeto and Mair methods, it can be found that the maximum surface settlement, S_{max}, occurs at the tunnel axis x, and the final values of S_{max} are 10.55 mm and 11.95 mm, respectively. These methods are more appropriate than that of Limanov's method (S_{max}=16.78 mm). While the maximum surface settlement in the monitoring of the field data measurements is 8 mm. On the other hand, the Ecrelebi method overestimates the settlements up to

S_{max}=26.23 mm. This causes to an uneconomic estimation and over design. In contrast, the Sagaseta method underestimates the settlement with the maximum of S_{max}=4.40 mm. The reason for the variation between the results of the different theoretical methods mentioned above is due to the assumptions and simplifications used in these relationships that neglect the influence of some factors, so that some cases give good results and disparate results in others. In spite of the theoretical methods have several advantages in the prediction of ground settlements induced by tunneling, there are major constraints in their practical application because the large number of influential factors involved makes tunnel–ground interaction complicated, it is difficult to say whether these methods can be used in confidence. In fact, there are some factors that are effect on the ground surface settlement which among; the geometry of tunnel (depth and diameter of the tunnel), tunnel construction method including; types of excavation and construction stages, and soil properties such as; poisson's ratio, friction angle, lateral earth pressure and ground water conditions. Therefore, most of empirical methods didn't take into consideration the effect of these parameters that play an important role in decision making for the proper selection of calculate the surface settlement.

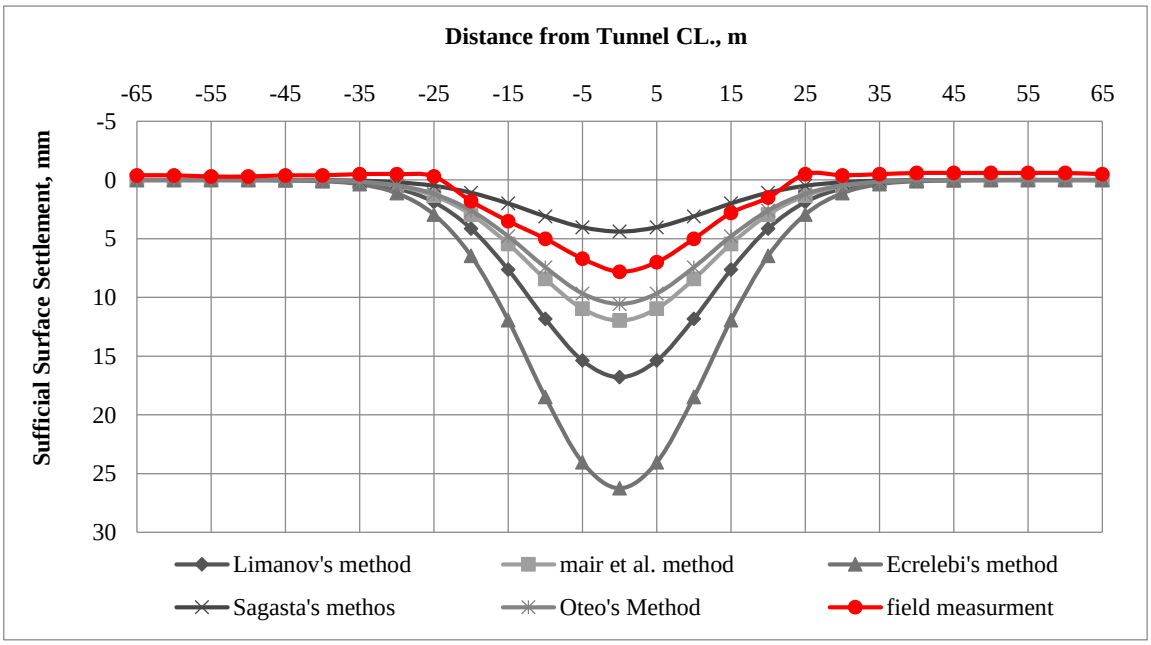

Figure 14. Transverse settlement trough of the ground surface

In the area close to the tunnel axis (−25 < x < 25 m), about 2.6 times of the excavation diameter, the theoretical results for Sagaseta, Oeto and Mair methods are larger than the measured result with an average value of about 3.00 mm, which means the theoretical prediction slightly overvalue the eventual surface settlement. The overvalues of theoretical results could be treated as the safety margin in a sensible way. In the area far away from the tunnel axis (x < −25 m and x > 25 m), the theoretical result is almost equal the measured result, which means the theoretical prediction slightly underestimates the eventual surface settlement. As all the measured results are smaller than 3.00 mm, the influence of the underestimation could be well accepted in the tunneling construction.

7. Conclusions

During the design and construction of the tunnels in urban areas, it is very necessary to predict the surface settlement to control the tunneling construction on an adjacent structure. Despite of unsuitability of the empirical methods for all different soil conditions and all variable site circumstances to calculate the ground surface displacements due to tunneling. However, it is preferable to using these methods for estimation of ground surface settlement due to tunnel construction are relatively simple procedures that are very often used in practice. They provide very good results when tunneling conditions are well known, i.e. when design parameters and soil calculation parameters are adequately calibrated. Main conclusions which could be deduced from the study performed, are listed below:

- The main advantage of using the theoretical methods that it can be used easily for different soil, where it just needs to substitute directly in the equation instead of using any charts.
- Good convergence in results for Oteo and Mair methods comparing with the field measurements where the maximum surface settlement ranges from 10.55-11.95 mm, respectively.
- A marginal agreement in results for Limanov's method comparing with the field measurements where the maximum surface settlement is 16.78 mm.

- A noticeable diversion in result for Ercelebi method comparing with the field measurements. Ercelebi method overestimates the settlements up to S_{max}=26.23 mm. This causes to an uneconomic estimation and over design. In contrast, the Sagaseta method underestimates the settlement with the maximum of S_{max} is 4.40 mm.

Finally, there are many factors that influence on the results accuracy such as; soil parameters and construction stages especially the loading and unloading behavior of soil that must be taken into account to measure the surface settlement. This paper presents the details of the project and monitoring results field and laboratory geotechnical investigations in order to determine the soil properties, which play a critical key role in the accuracy of results. Consequently, by numerical simulation the effects of tunneling construction on surface settlement and piles foundation are the scope of interest for future research.

8. Funding

The publishing of this paper is financially supported by the National Natural Science Foundation of China (No. 11672215).

9. Conflicts of Interest

The authors declare no conflict of interest.

10. References

[1] Hefny, Ashraf, Mohamed Ezzat Al-Atroush, Mai Abualkhair, and Mariam Juma Alnuaimi. "Three-Dimensional Response of the Supported-Deep Excavation System: Case Study of a Large Scale Underground Metro Station." Geosciences 10, no. 2 (February 19, 2020): 76. doi:10.3390/geosciences10020076.

[2] Attewell, P.B., and I.W. Farmer. "Ground Disturbance Caused by Shield Tunnelling in a Stiff, Overconsolidated Clay." Engineering Geology 8, no. 4 (December 1974): 361–381. doi:10.1016/0013-7952(74)90028-3.

[3] Basile, Francesco. "Effects of Tunnelling on Pile Foundations." Soils and Foundations 54, no. 3 (June 2014): 280–295. doi:10.1016/j.sandf.2014.04.004.

[4] Park, Kyung-Ho. "Analytical Solution for Tunnelling-Induced Ground Movement in Clays." Tunnelling and Underground Space Technology 20, no. 3 (May 2005): 249–261. doi:10.1016/j.tust.2004.08.009.

[5] Ercelebi, S. G., H. Copur, and I. Ocak. "Surface Settlement Predictions for Istanbul Metro Tunnels Excavated by EPB-TBM." Environmental Earth Sciences 62, no. 2 (March 27, 2010): 357–365. doi:10.1007/s12665-010-0530-6.

[6] Zhang, Zhiguo, Maosong Huang, Chengping Zhang, Kangming Jiang, and Minghao Lu. "Time-Domain Analyses for Pile Deformation Induced by Adjacent Excavation Considering Influences of Viscoelastic Mechanism." Tunnelling and Underground Space Technology 85 (March 2019): 392–405. doi:10.1016/j.tust.2018.12.020.

[7] Wang, Hongyu, Chun Fai Leung, Jian Yu, and Maosong Huang. "Axial Response of Short Pile Due to Tunnelling-Induced Soil Movement in Soft Clay." International Journal of Physical Modelling in Geotechnics 20, no. 2 (March 2020): 71–82. doi:10.1680/jphmg.18.00045.

[8] Ambooken, Akhil, R. K. Madhumathi, and K. Ilamparuthi. "Response of Single Pile Due to Deep Excavation and Underground Openings." Geotechnical Applications (June 13, 2018): 261–269. doi:10.1007/978-981-13-0368-5_28.

[9] Darvishpour, Alireza, Asadollah Ranjbar, and Amirmohammad Amiri. "The Effect of Soil Reinforcement on the Stress and Strain Field Around Underground Square-Shaped Areas and Its Internal Lining Efforts in Urban Areas." Civil Engineering Journal 4, no. 11 (November 30, 2018): 2756. doi:10.28991/cej-03091196.

[10] Barla, Marco, Claudia Klotz, and Ina Valodzka. "Scenario analysis of risk-oriented design for geotechnical structures." (2018).

[11] Atkinson, J. H., and D. M. Potts. "Subsidence Above Shallow Tunnels in Soft Ground." International Journal of Rock Mechanics and Mining Sciences & Geomechanics Abstracts 14, no. 4 (July 1977): 65. doi:10.1016/0148-9062(77)91056-7.

[12] Huang, H, H Bao, and D Zhang. "A Complex Variable Solution for Tunneling-Induced Ground Movements in Clays." Geotechnical Aspects of Underground Construction in Soft Ground (December 9, 2008). doi:10.1201/9780203879986.ch105.

[13] Attewell, Peter B., John Yeates, and Alan R. Selby. "Soil Movements Induced by Tunnelling and Their Effects on Pipelines and Structures." Tunnelling and Underground Space Technology 2, no. 1 (January 1987): 102. doi:10.1016/0886-7798(87)90195-7.

[14] Peck, R.B. "State-of-the-art: Deep excavation and tunneling in soft ground." Proceedings of the Seventh International Conference on Soil Mechanics and Foundation Engineering, Universidad Nacional Autonoma de Mexico Instituto de Ingenira,1969, Mexico City, Mexico, Vol. 3, pp. 225-290.

[15] Burland, J. B., Broms, B. B., and de Mello, V. F. B. "Behavior of foundations and structures." State-of-the-Art Report. Proc, 9th Int. Conf. on Soil Mech. and Found. Engr., II, Tokyo, Japan, (1977): 495-546.

[16] Rankin, W. J. "Ground Movements Resulting from Urban Tunnelling: Predictions and Effects." Geological Society, London, Engineering Geology Special Publications 5, no. 1 (1988): 79–92. doi:10.1144/gsl.eng.1988.005.01.06.

[17] Boscardin, Marco D., and Edward J. Cording. "Building Response to Excavation-Induced Settlement." International Journal of Rock Mechanics and Mining Sciences & Geomechanics Abstracts 26, no. 3–4 (July 1989): A225. doi:10.1016/0148-9062(89)92930-6.

[18] Ahmed, S. M. "State-of-the-art report: deformations associated with deep excavation and their effects on nearby structures." Ain Shams University, Cairo, (2014): 164.

[19] National Authority for tunnel. "Tunnel from Attaba to Geish shaft monitoring measurements", contract N 49/Metro, phase 1", Greater Cairo Metro, (2010): 270-271.

[20] Hamza Associates. "Geotechnical investigation report: Greater Cairo Metro-Line 3". (2002).

[21] ECP 202/1. 2005. "Egyptian code for soil mechanics – design and construction of foundations." Part 1, Site investigation. The Housing and Building Research Center (HBRC), Cairo, Egypt.

[22] Peck, Ralph Brazelton., Walter Edmund Hanson, and Thomas Hampton. Thornburn. "Foundation Engineering." Soil Science 75, no. 4 (April 1953): 329. doi:10.1097/00010694-195304000-00012.

[23] Giuliani, F., and F. L. Nicoll. "New analytical correlations between SPT, overburden pressure and relative density." Proceedings of 2nd European symposium on penetration testing, Amsterdam (1982).

[24] Wolff, Thomas F. "Pile capacity prediction using parameter functions." Predicted and Observed Axial Behavior of Piles: Results of a Pile Prediction Symposium. ASCE, (1989).

[25] Webb, D.L. "Settlement of Structures on Deep Alluvial Sandy Sediments in Durban, South Africa." Proceedings of the Conference on In Situ Investigations in Soils and Rocks, BGS., (1969): 181-187.

[26] Bowles, J.E. "Foundation Analysis and Design." 3rd Ed., McGraw Hill, Inc., New York, (1982).

[27] Denver. H. "Modulus of Elasticity for Sand Determined by SPT and CPT." Proceedings of the 2nd European Symposium on Penetration Testing, Vol. I, (1982): 35-40.

[28] ECP 202/3. "Egyptian code for soil mechanics – design and construction of foundations." Part 3, Shallow Foundation. The Housing and Building Research Center (HBRC), Cairo, Egypt, (2005).

[29] Hazen, Allen. "Some physical properties of sands and gravels: with special reference to their use in filtration." State Sanitation Volume II (2013). doi:10.4159/harvard.9780674600485.c25.

[30] ECP 202/2. "Egyptian code for soil mechanics – design and construction of foundations." Part 2, Laboratory tests. The Housing and Building Research Center (HBRC), Cairo, Egypt, (2005).

[31] Duncan, James Moyer, and A. L. Buchignani. "An Engineering Manual for Settlement Studies": By JM Duncan and AL Buchignani. Department of Civil Engineering, University of California, (1976).

[32] Mair, R. J., M. J. Gunn, and M. P. O'REILLY. "Ground Movement around Shallow Tunnels in Soft Clay." International Journal of Rock Mechanics and Mining Sciences & Geomechanics Abstracts 19, no. 6 (December 1982): 141. doi:10.1016/0148-9062(82)91516-9.

[33] O'Reilly, M.P., and B.M. New. "Settlement above Tunnels in the United Kingdom — Their Magnitude and Prediction." International Journal of Rock Mechanics and Mining Sciences & Geomechanics Abstracts 20, no. 1 (February 1983): A18. doi:10.1016/0148-9062(83)91768-0.

[34] Mair, R. J., and R. N. Taylor. "Theme lecture: Bored tunnelling in the urban environment." Proceedings of the fourteenth international conference on soil mechanics and foundation engineering. Rotterdam, (1997).

[35] Oteo, C., and J. F. Moya. "Evaluación de parámetros del suelo de Madrid con relación a la construcción de túneles." In: Proceedings of the 7th European Conference on Soil Mechanics and Foundation Engineering, Brighton. Vol. 3, No. 13, (1979): 239-247.

[36] Sagaseta, C., J. F. Moya, and C. Oteo. "Estimation of ground subsidence over urban tunnels." 2nd Int. Conf. "Ground movements and structure. (1980): 331-345.

[37] Limaniv, J. A. "Infolge Tunnelbau in kambrischen Tonen Leningrad Inst-Inzh." Zhelezu, Transport (1957).

[38] Sagaseta, C. "Analysis of Undraind Soil Deformation Due to Ground Loss." Géotechnique 37, no. 3 (September 1987): 301–320. doi:10.1680/geot.1987.37.3.301.

[39] Sagaseta, C. "Discussion: Analysis of Undrained Soil Deformation Due to Ground Loss." Géotechnique 38, no. 4 (December 1988): 647–649. doi:10.1680/geot.1988.38.4.647.

[40] Uriel, A.O., and Sagaseta, C. "Selection of design parameters for underground construction." In Proceedings of the 12th International Congress on Soil Mechanics, Río de Janeiro, 13–18 August, 1989, General report, Discussion session. A.A. Balkema, Rotterdam. Vol. 9, (1989): 2521–2551.

[41] Ercelebi, S. G., et al. "Surface settlement prediction for Istanbul metro tunnels via 3D FE and empirical methods." Tunneling and Underground Space Technology, London, England (2005): 163-169.